ERNEST ORLANDO LAWRENCE BERKELEY NATIONAL LABORATORY

A Statistical Interpretation of the Correlation Between IMF Multiplicity and Transverse Energy

L. Phair, L. Beaulieu, L.G. Moretto, G.J. Wozniak,
D.R. Bowman, N. Carlin, L. Celano, N. Colonna,
J.D. Dinius, A. Ferrero, C.K. Gelbke, T. Glasmacher,
F. Gramegna, D.O. Handzy, W.C. Hsi, M.J. Huang, I. Iori,
Y.D. Kim, M.A. Lisa, W.G. Lynch, G.V. Margagliotti,
P.F. Mastinu, P.M. Milazzo, C.P. Montoya, A. Moroni,
G.F. Peaslee, R. Rui, C. Schwarz, M.B. Tsang, K. Tso,
G. Vannini, and F. Zhu

Nuclear Science Division

June 1998

DISCLAIMER

A Statistical Interpretation of the Correlation Between IMF Multiplicity and Transverse Energy

L. Phair,[1] L. Beaulieu,[1] L.G. Moretto,[1] G.J. Wozniak,[1] D.R. Bowman,[2] N. Carlin,[3]
L. Celano,[5] N. Colonna,[5] J.D. Dinius,[2] A. Ferrero,[3] C.K. Gelbke,[2] T. Glasmacher,[2]
F. Gramegna,[6] D.O. Handzy,[2] W.C. Hsi,[2] M.J. Huang,[2] I. Iori,[3] Y.D. Kim,[2]
M.A. Lisa,[2] W.G. Lynch,[2] G.V. Margagliotti,[4] P.F. Mastinu,[7] P.M. Milazzo,[7]
C.P. Montoya,[2] A. Moroni,[3] G.F. Peaslee,[2] R. Rui,[4] C. Schwarz,[2] M.B. Tsang,[2]
K. Tso,[1] G. Vannini,[4] and F. Zhu[2]

[1]Nuclear Science Division, Ernest Orlando Lawrence Berkeley National
Laboratory, University of California, Berkeley, California 94720
[2]National Superconducting Cyclotron Laboratory and Department of Physics and
Astronomy, Michigan State University, East Lansing, Michigan 48824
[3]Istituto Nazionale di Fisica Nucleare and Dipartimento di Fisica,
Via Celoria 16, 20133 Milano, Italy
[4]Dipartimento di Fisica and Istituto Nazionale di Fisica Nucleare,
Via A. Valerio 2, 34127 Trieste, Italy
[5]Istituto Nazionale di Fisica Nucleare, Via Amendola 173, 70126 Bari, Italy
[6]Istituto Nazionale di Fisica Nucleare, Laboratori Nazionali di Legnaro,
Via Romea 4, 35020 Legnaro, Italy
[7]Dipartimento di Fisica and Istituto Nazionale di Fisica Nucleare, Bologna, Italy

June 1998

A statistical interpretation of the correlation between IMF multiplicity and transverse energy

L. Phair[1], L. Beaulieu[1], L.G. Moretto[1], G.J. Wozniak[1], D. R. Bowman[2,*], N. Carlin[2,†], L. Celano[5], N. Colonna[5], J.D. Dinius[2], A. Ferrero[3], C.K. Gelbke[2], T. Glasmacher[2], F. Gramegna[6], D.O. Handzy[2], W.C. Hsi[2], M.J. Huang[2], I. Iori[3], Y.D. Kim[2,§], M.A. Lisa[2,∥], W.G. Lynch[2], G.V. Margagliotti[4], P.F. Mastinu[7,¶], P.M. Milazzo[7,¶], C.P. Montoya[2], A. Moroni[3], G.F. Peaslee[2,**], R. Rui[4], C. Schwarz[2], M.B. Tsang[2], K. Tso[1], G. Vannini[4], F. Zhu[2]

[1] Nuclear Science Division, Lawrence Berkeley National Laboratory, Berkeley, California 94720
[2] National Superconducting Cyclotron Laboratory and Department of Physics and Astronomy, Michigan State University, East Lansing, MI 48824
[3] Istituto Nazionale di Fisica Nucleare and Dipartimento di Fisica, Via Celoria 16, 20133 Milano, Italy
[4] Dipartimento di Fisica and Istituto Nazionale di Fisica Nucleare, Via A. Valerio 2, 34127 Trieste, Italy
[5] Istituto Nazionale di Fisica Nucleare, Via Amendola 173, 70126 Bari, Italy
[6] Istituto Nazionale di Fisica Nucleare, Laboratori Nazionali di Legnaro, Via Romea 4, 35020 Legnaro, Italy
[7] Dipartimento di Fisica and Istituto Nazionale di Fisica Nucleare, Bologna, Italy

(June 1, 1998)

Multifragment emission following ^{129}Xe+^{197}Au collisions at 30, 40, 50 and 60 AMeV has been studied with multidetector systems covering nearly 4π in solid angle. The correlations of both the intermediate mass fragment and light charged particle multiplicities with the transverse energy are explored. A comparison is made with results from a similar system, ^{136}Xe+^{209}Bi at 28 AMeV. The experimental trends are compared to statistical model predictions.

Highly excited nuclear matter can be produced in intermediate-energy heavy-ion collisions. In these reactions, its decay by intermediate mass fragment (IMF: $3 \leq Z \leq 20$) emission is observed [1]. The mechanism causing multifragment decay is not yet fully understood and is a subject of current debate. Some have argued that multifragmentation is a dynamical process [2,3]. Others have interpreted the IMFs produced in similar systems as being predominantly statistical in origin [4-9]. These disagreements are centered around the interpretation of IMF multiplicity (N_{IMF}) data and their correlation with a particular measure of the violence of the collision, the transverse energy E_t (defined as $E_t = \sum_i E_i \sin^2 \theta_i$, where the kinetic energies E of all charged particles in an event are weighted by the sine squared of their polar angles θ and summed).

In recent papers, Toke *et al.* have offered a new interpretation regarding the origin of the correlation between N_{IMF} and E_t. In one study [2], these authors explored the dependence of the light charged particle multiplicity (N_{LCP}), the transverse energy of LCPs (E_t^{LCP}), and the transverse energy of IMFs (E_t^{IMF}) as a function of N_{IMF}. Based upon their analysis, they concluded that a new mode of energy dissipation is present and that the resulting IMFs are formed dynamically. In another study [3], the authors examined the contributions to E_t from IMFs and LCPs, and from their analysis, they ruled out

TABLE I. Values are given for the approximate N_{IMF} saturation value (along with the upper limit of the integrated cross section in percent which this represents), the average LCP multiplicity and average E_t^{LCP} in the saturation region of Fig. 1, and the maximum average IMF multiplicity for the top 5% of the E_t selected events, all from the reaction ^{129}Xe+^{197}Au at the indicated bombarding energies.

E_{beam}/A	$N_{\mathrm{IMF}}^{\mathrm{sat}}$	$\langle N_{\mathrm{LCP}} \rangle_{\mathrm{max}}$	$\left\langle E_t^{\mathrm{LCP}} \right\rangle_{\mathrm{max}}$	$\langle N_{\mathrm{IMF}} \rangle_{\mathrm{max}}$
30 MeV	5 (6.5%)	13.9	220 MeV	4.6
40 MeV	7 (5.0%)	18.9	400 MeV	6.0
50 MeV	8 (4.3%)	23.1	530 MeV	6.9
60 MeV	8 (5.9%)	26.1	660 MeV	7.4

statistical emission as a possible origin of the IMFs.

We have reviewed their conclusions and have found that many of their observations can be reproduced by statistical models. We have also found that the results from ref. [3] are inconsistent with measurements taken with a detector of improved dynamical range. Therefore, the interpretation in [3] is probably in error.

In what follows we report on 1) the general nature of the observations of refs. [2,3]; 2) the limited usefulness of gating on N_{IMF} as an event-selection strategy; 3) experimental acceptance issues which introduce artificially features similar to those observed in ref. [3]; and 4) the reproduction of key results with statistical model calculations.

Our measurements of the LCP and IMF yields and their correlations with, and contributions to E_t were made for the reaction ^{129}Xe+^{197}Au at 30, 40, 50, and 60 AMeV. The experiments were performed at the National Superconducting Cyclotron Laboratory at Michigan State University (MSU). Beams of ^{129}Xe, at intensities of about 10^7 particles per second, irradiated gold targets of approximately 1 mg/cm^2. LCPs and IMFs produced in these reactions were measured with the MSU Miniball phoswich array [10]. For the bombarding en-
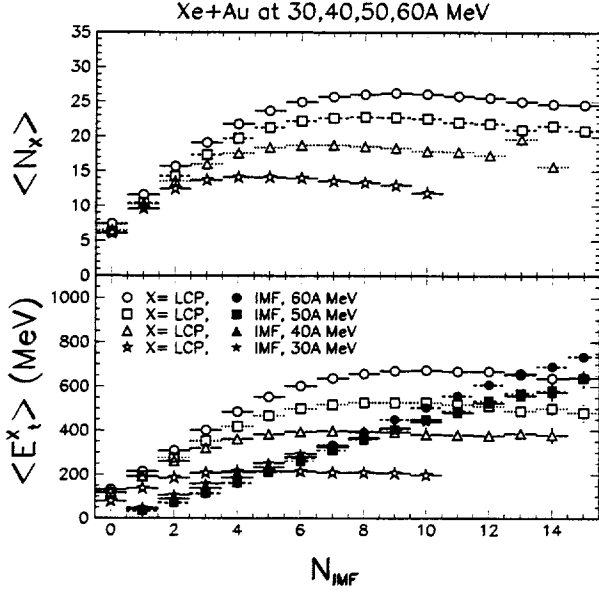
FIG. 1. The average LCP multiplicity (top panel), average transverse energy of IMFs (solid symbols), and average E_t of LCPs (open symbols, bottom panel) are plotted as a function of IMF multiplicity for the reaction ^{129}Xe+^{197}Au at bombarding energies between 30 and 60 AMeV.

ergies of 40, 50 and 60 AMeV, the particles going forward ($\leq 16°$) were measured with the LBL forward array [11], a high resolution Si-Si(Li)-plastic scintillator array. For the 30 AMeV data set, the forward going particles ($\leq 23°$) were measured by the MULTICS array [12], a high resolution gas-Si-Si(Li)-CsI array. Details of the experimental setups can be found in refs. [13,14].

We now investigate the advantages and disadvantages of using N_{IMF} as a global event selector, as employed in ref. [2], to determine the average LCP yields as a function of impact parameter or energy deposition. Fig. 1 shows an example of such an analysis for the reaction ^{129}Xe+^{197}Au at bombarding energies between 30 and 60 AMeV. The average LCP multiplicity ($\langle N_{\mathrm{LCP}} \rangle$) saturates in a bombarding energy dependent fashion (top panel). The value to which $\langle N_{\mathrm{LCP}} \rangle$ saturates ($\langle N_{\mathrm{LCP}} \rangle_{\max}$) rises with increasing bombarding energy and is listed in Table I. The IMF multiplicity at which the saturation occurs is approximately 4-5 at 30 AMeV and rises with increasing bombarding energy to a value of 8-9 at 60 AMeV. The average LCP contribution to E_t ($\langle E_t^{\mathrm{LCP}} \rangle$) saturates in a bombarding energy dependent fashion as well (see $\langle E_t^{\mathrm{LCP}} \rangle_{\max}$ in Table I and open symbols of Fig. 1, bottom panel). In contrast, the average IMF contribution to E_t ($\langle E_t^{\mathrm{IMF}} \rangle$) rises with increasing IMF multiplicity since

$$\langle E_t^{\mathrm{IMF}} \rangle = \left\langle \sum_{i=1}^{N_{\mathrm{IMF}}} E_i \sin^2 \theta_i \right\rangle \approx N_{\mathrm{IMF}} \langle \epsilon_t^{\mathrm{IMF}} \rangle, \quad (1)$$

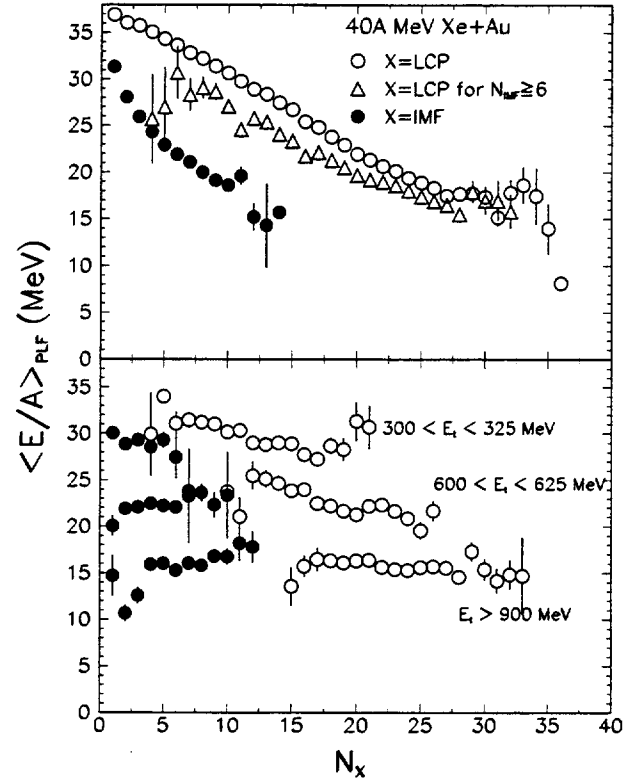where $\langle \epsilon_t^{\mathrm{IMF}} \rangle$ is the average transverse energy of an IMF.

FIG. 2. Top panel: the average kinetic energy per nucleon of the projectile-like fragment is plotted as a function of N_{IMF} (solid circles) and N_{LCP} (open symbols). Bottom panel: Same as top panel but selected from events within the indicated range of E_t.

The trends shown in Fig. 1 for ^{129}Xe+^{197}Au confirm the general nature of similar observations for Xe+Bi at 28 AMeV [2]. Furthermore, a clear bombarding energy dependence is observed, with larger saturation values (as a function of N_{IMF}) of $\langle N_{\mathrm{LCP}} \rangle_{\max}$ and $\langle E_t^{\mathrm{LCP}} \rangle_{\max}$ for increasing bombarding energy.

It has been argued that the saturation of the LCP observables (as opposed to the continuous rise of $\langle E_t^{\mathrm{IMF}} \rangle$) as a function of N_{IMF} provides supporting evidence for dynamical fragment production. The claim is that such a saturation helps demonstrate that the IMFs do not compete statistically for the available thermal energy [2].

As complementary evidence, the dependence of the average kinetic energy of the projectile-like fragment ($\langle E/A \rangle_{\mathrm{PLF}}$), defined as the heaviest forward-moving particle in an event, with $Z_{\mathrm{PLF}} \geq 10$ and $\theta \leq 23°$) has been studied as a function of N_{IMF}, an example of which is given in Fig. 2 for ^{129}Xe+^{197}Au at 40 AMeV (solid circles). From the decrease of $\langle E/A \rangle_{\mathrm{PLF}}$ with N_{IMF}, the authors of ref. [2] concluded that kinetic energy of the PLF is being expended for the production of IMFs. It was also argued that for increasing N_{IMF}, the saturation of $\langle N_{\mathrm{LCP}} \rangle$ represents a critical excitation energy value beyond which no further amount of relative kinetic energy between the PLF and TLF is converted into heat.
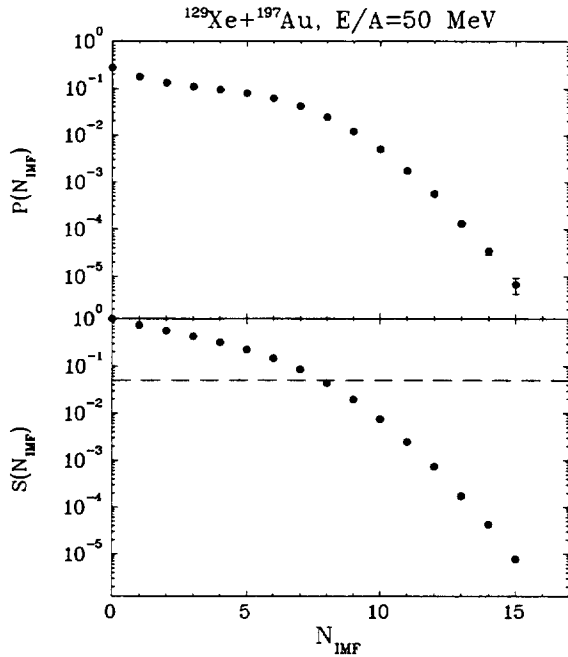
2

FIG. 3. Top panel: Probability to emit N_{IMF} from the reaction $^{129}\mathrm{Xe}+^{197}\mathrm{Au}$ at 50 AMeV. Bottom panel: Integrated probability to emit N_{IMF} or more IMFs.

In other words, the IMFs no longer compete with the LCPs for the available energy – they get it all. It was this observation, together with data like those in Fig. 1, that was taken as evidence for dynamical emission [2].

One can test the consistency of such an explanation by studying the same observable, $\langle E/A\rangle_{\mathrm{PLF}}$, but now as a function of N_{LCP} (open symbols, top panel of Fig. 2). We observe the same dependence as that of the IMFs – a monotonic decrease of $\langle E/A\rangle_{\mathrm{PLF}}$ with increasing N_{LCP} which reaches a value of ~17 MeV at the largest multiplicities. This behaviour persists whether we restrict ourselves to the saturation region ($N_{\mathrm{IMF}}\geq 6$, triangles) or not (open circles). It seems that the LCPs do in fact "cost" energy (as measured by the PLF) and therefore do compete with the IMFs for the available energy.

This can be seen more clearly by pre-selecting events with a better global observable, E_t [15–17], as done in the bottom panel of Fig. 2. Once a window of E_t is selected, a corresponding value of $\langle E/A\rangle_{\mathrm{PLF}}$ is also determined, and there is no longer any strong dependence of $\langle E/A\rangle_{\mathrm{PLF}}$ on N_{IMF} or N_{LCP}. In fact, the resulting N_{IMF} and N_{LCP} selections both give the *same* value of $\langle E/A\rangle_{\mathrm{PLF}}$, consistent with a scenario where both species compete for the same available energy.

What then causes the saturation observed in Fig. 1? It is the discreteness and limited range of N_{IMF} along with its weak correlation to the deposited energy.

For example, when compared to the total charged particle multiplicity $N_C=N_{\mathrm{IMF}}+N_{\mathrm{LCP}}$, it is obvious that $N_{\mathrm{IMF}}\leq N_C$ and therefore $\Delta N_{\mathrm{IMF}}/N_{\mathrm{IMF}}\geq \Delta N_C/N_C$ where $\Delta N_{\mathrm{IMF}}=\Delta N_C=1$, the base unit of change of these
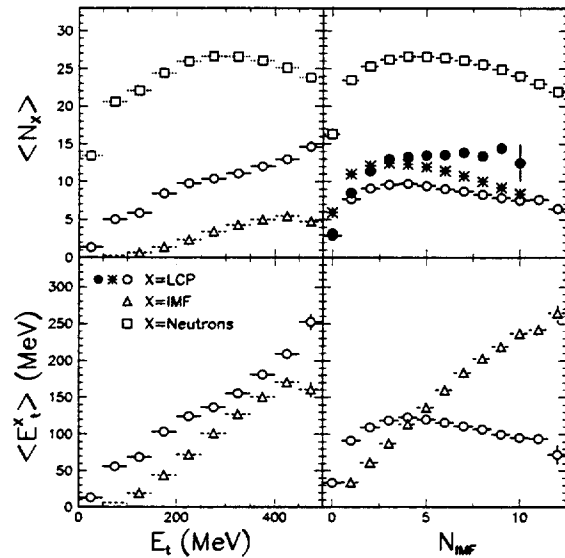

FIG. 4. Statistical model predictions from SMM (open symbols), percolation (solid symbols), and the simple model described in the text (crossed symbols). Upper left: the predicted average LCP and IMF multiplicities are plotted as a function of E_t for the decay of an ensemble of gold nuclei with excitation energies between 0.5-6.0 AMeV. Upper right: the average LCP and neutron multiplicities are plotted as a function of N_{IMF}. Lower left: the average E_t of the LCPs and IMFs as a function of E_t is shown. Lower right: the average E_t of the LCPs and IMFs is shown as a function of N_{IMF}.

observables. Consequently, any measure of energy deposition or centrality of the collision based upon N_{IMF} will lead to much larger fluctuations in the deduced impact parameter scale than one based on, for example, N_C [15].

Furthermore, the values of N_{IMF} at which the observables in Fig. 1 saturate ($N_{\mathrm{IMF}}^{\mathrm{sat}}$) can be understood in terms of such an impact parameter scale. Consider the probability P of emitting N_{IMF} and its integrated yield

$$S(N_{\mathrm{IMF}}) = \sum_{i=N_{\mathrm{IMF}}}^{\infty} P(i) \qquad (2)$$

as shown in Fig. 3 for the reaction $^{129}\mathrm{Xe}+^{197}\mathrm{Au}$ at 50 AMeV. Average impact parameter scales, as they are commonly employed, are proportional to $\sqrt{S}$ [15]. We note that the multiplicities at which saturation occurs represent roughly 5% of the total integrated cross section (dashed line in the bottom panel of Fig. 3). The N_{IMF} value $N_{\mathrm{IMF}}^{\mathrm{sat}}$ for which $S \approx 0.05$ is listed in Table I for each of the different bombarding energies. $N_{\mathrm{IMF}}^{\mathrm{sat}}$ tracks rather well the maximum average N_{IMF} ($\langle N_{\mathrm{IMF}}\rangle_{\mathrm{max}}$) measured for the most central collisions (top 5% of events) based upon the E_t scale.

The above observations demonstrate that large IMF multiplicities ($N_{\mathrm{IMF}}>\langle N_{\mathrm{IMF}}\rangle_{\mathrm{max}}$) have small probabilities and represent the extreme tails of events associated with the most central collisions. In other words, events
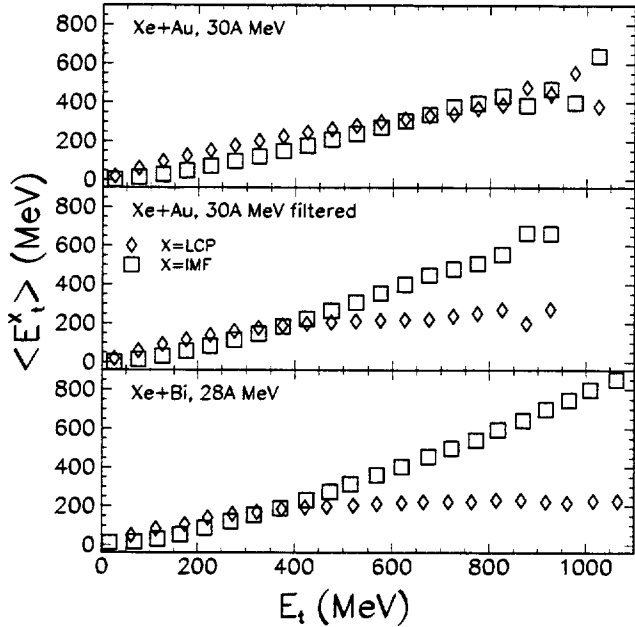
3

FIG. 5. The average transverse energies of IMFs (squares) and of LCPs (diamonds) are plotted as a function of E_t for the reactions ^{129}Xe+^{197}Au at 30 AMeV (top panel), ^{129}Xe+^{197}Au again but filtered with the upper energy thresholds of the dwarf array detector [21] (middle panel), and ^{136}Xe+^{209}Bi at 28 AMeV (bottom panel, taken from ref. [3]).
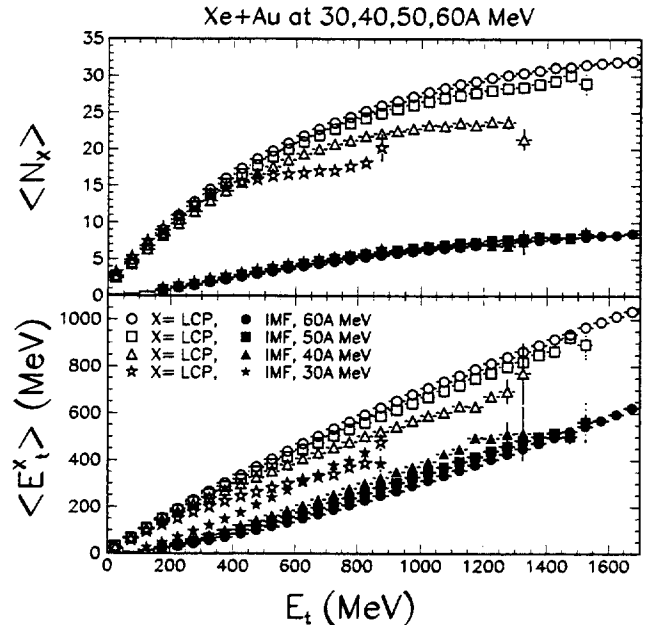

FIG. 6. The average IMF multiplicity (solid symbols, top panel), average LCP multiplicity (open symbols, top panel), average transverse energy of IMFs (solid symbols, bottom panel), and average transverse energy of LCPs (open symbols, bottom panel) are plotted as a function of E_t for the reaction ^{129}Xe+^{197}Au at the indicated bombarding energies.

with increasing values of N_{IMF} in the saturation region of Fig. 1 do not come from events where more energy has been dissipated. Thus, N_{IMF} is useful as a global event selector over only a very limited range.

Consequently, it is expected that statistical models should exhibit similar trends as observed in Fig. 1. Examples of such predictions are shown in Fig. 4 for the statistical multifragmentation model SMM (open symbols) [18] and for percolation (solid symbols) [19]. In both models an excitation energy (E) distribution was used such that the number of events at a given E was proportional to ($E_{max} - E$) where E_{max} is the largest calculated excitation energy. The "excitation energy" for the percolation calculation is essentially represented by the number of broken bonds and is calculated as per ref. [19].

Both calculations show a saturation of $\langle N_{LCP} \rangle$ when plotted as a function of N_{IMF}. This behavior can be understood in terms of a simple model. Consider the statistical emission of two particle types with barriers B_1 and B_2 (and $B_2 > B_1$). Assume the emission probabilities are $p_i \propto \exp[-B_i/T]$ ($i = 1, 2$) with $p_1 + p_2 = 1$. With the temperature T characterized in terms of the total multiplicity $n_{tot} = n_1 + n_2 = \alpha T$, and ignoring mass conservation, the solution for $\langle n_1 \rangle$ as a function of n_2 can be calculated for a distribution of excitation energies like that described above. The solution of this model is shown by the crossed symbols in the top right panel of Fig. 4 for $B_1=8$, $B_2=24$, $T_{max}=10$ and $\alpha = 2$ (and

$N_{IMF}=n_2$, $N_{LCP}=n_1$). This behavior is similar to that of the other statistical models listed in Fig. 4 and to the behavior observed in Fig. 1. This behavior is a generic feature that is present in any statistical model [20]. The saturation comes about because N_{IMF} is a poor measure of the "excitation energy", as mentioned previously.

Up to this point, we have offered alternative explanations for the similar behaviors observed in N_{IMF} selected studies of ^{129}Xe+^{197}Au and ^{136}Xe+^{209}Bi. In the remainder of this paper we focus on the observed differences between these reactions when other event selection strategies are employed.

When using a different global observable (E_t), an unusual behavior of the E_t selected events appears in the measured ^{136}Xe+^{209}Bi reaction [3]. The contribution to E_t from IMFs and LCPs is shown in the bottom panel of Fig. 5 for the reaction ^{136}Xe+^{209}Bi. Of particular note is the strong saturation observed for $\langle E_t^{LCP} \rangle$ (diamonds). This was taken to indicate a decoupling or a loss of statistical competition between the IMFs and LCPs [3].

However, in a similar reaction, ^{129}Xe+^{197}Au, the saturation observed in ^{136}Xe+^{209}Bi is not present. In Fig. 6 are plotted $\langle N_{IMF} \rangle$, $\langle N_{LCP} \rangle$, $\langle E_t^{IMF} \rangle$, and $\langle E_t^{LCP} \rangle$ as a function of E_t for bombarding energies between 30 and 60 AMeV. Neither $\langle N_{LCP} \rangle$ nor $\langle E_t^{LCP} \rangle$ saturate at any value of E_t. And, unlike the measurement for ^{136}Xe+^{209}Bi, the IMFs measured in the ^{129}Xe+^{197}Au reactions are never the dominant carrier of E_t.

4

We believe that the saturation observed in ref. [3] (see bottom panel of Fig. 5) is likely due to the limited dynamic range of the detectors used. The charged particle yields from the ^{136}Xe+^{209}Bi reaction were measured with the dwarf array [21] whose thin CsI crystals (thickness of 4 mm for polar angle $\theta = 55-168°$, 8mm for $\theta = 32-55°$ and 20 mm for $\theta = 4-32°$) are unable to stop energetic LCPs. For example, protons punch through 4 mm of CsI at an energy of 30 MeV. Consequently, their contribution to E_t could be significantly underestimated.

An example of the distortions that would be caused by the detector response of the dwarf array on the similar ^{129}Xe+^{197}Au reaction at 30 AMeV is given in Fig. 5. In the top panel is plotted $\langle E_t^{\mathrm{LCP}} \rangle$ and $\langle E_t^{\mathrm{IMF}} \rangle$ as a function of E_t as measured by the MULTICS/Miniball collaboration. The thicknesses of the CsI crystals from these detectors range from 20 to 40 mm. Protons punch through 20 mm of CsI with an energy of 76 MeV. In the middle panel of Fig. 5, the ^{129}Xe+^{197}Au data has been "filtered" using the dwarf array high energy cutoffs which remove high energy particles from E_t. After filtering, the two prominent features observed in the ^{136}Xe+^{209}Bi data set [3] (bottom panel of Fig. 5) then appear in the filtered data. Namely, $\langle E_t^{\mathrm{LCP}} \rangle$ saturates to a small value and $\langle E_t^{\mathrm{IMF}} \rangle$ becomes the "apparent" dominant carrier of E_t. These two features are likely to be instrumental in origin and therefore do not warrant a physical interpretation. Consequently, they do not represent evidence of a failure of statistical models.

For example, the SMM calculations in Fig. 4 (lower left panel) show no hint of saturation of $\langle E_t^{\mathrm{LCP}} \rangle$ with increasing E_t. Instead, this calculation shows qualitatively the same trends as experimentally observed in Fig. 6.

In summary, the saturations observed in $\langle N_{\mathrm{LCP}} \rangle$ and $\langle E_t^{\mathrm{LCP}} \rangle$ as a function of N_{IMF} are fundamental features of statistical decay [20] rather than evidence for dynamical emission. A bombarding energy dependence of $\langle N_{\mathrm{LCP}} \rangle$, $\langle E_t^{\mathrm{LCP}} \rangle$, and $N_{\mathrm{IMF}}^{\mathrm{sat}}$ is expected (and experimentally observed) within the framework of statistical decay. Furthermore, it has been demonstrated that the LCPs compete with the IMFs for the available energy. By using E_t, a more sensitive event selection is obtained which demonstrates the limited usefulness of event classification using N_{IMF}. The saturation of $\langle E_t^{\mathrm{LCP}} \rangle$ as a function of E_t observed in ref. [3] is likely due to instrumental distortions. We can account for this saturation by filtering the present measurements of ^{129}Xe+^{197}Au with the experimental thresholds present in refs. [2,3]. The resulting distortions to the data are large and induce qualitative changes in the trends of the data, causing an unphysical saturation of $\langle E_t^{\mathrm{LCP}} \rangle$. Therefore, the observations listed in refs. [2,3] do not demonstrate any measurable failure of statistical models that would justify invoking dynamical IMF production by default. While the IMFs may indeed be produced dynamically, the observations listed in refs. [2,3] do not provide credible evidence for such a conclusion.

Present addresses:
* Washington Aerial Measurements Operations, Bechtel Nevada, P.O. Box 380, Suitland, MD 20752
† Instituto de Fisica, Universidade de Sao Paulo, C.P. 66318, CEP 05389-970, Sao Paulo, Brazil
§ Physics Department, Seoul National University, Seoul, 151-742, Korea.
‖ Physics Department, Ohio State University, Columbus, OH 43210
¶ Dipartimento di Fisica and Istituto Nazionale di Fisica Nucleare, Via A. Valerio 2, 34127 Trieste, Italy
**Physics Department, Hope College, Holland, MI 49423

[1] L.G. Moretto and G.J. Wozniak, Annu. Rev. Nucl. & Part. Sci. 43, 379 (1993).
[2] J. Toke et al., Phys. Rev. Lett. 77, 3514 (1996).
[3] J. Toke et al., Phys. Rev. C56, R1683 (1997).
[4] L.G. Moretto et al., Phys. Rev. Lett. 74, 1530 (1995).
[5] K. Tso et al., Phys. Lett. B 361, 25 (1995).
[6] L. Phair et al., Phys. Rev. Lett. 75, 213 (1995).
[7] M. D'Agostino et al., Phys. Lett. B 371, 175 (1996).
[8] L.G. Moretto, et al., Phys. Rep. 287, 249 (1997).
[9] L. Beaulieu et al., LBNL report 41075, submitted to Phys. Rev. Lett.
[10] R.T. De Souza et al., Nucl. Inst. Meth. A295, 109 (1990).
[11] W.L. Kehoe et al., Nucl. Inst. Meth. A311, 258 (1992).
[12] I. Iori et al., Nucl. Inst. Meth. A325, 458 (1993).
[13] D.R. Bowman et al., Phys. Rev. C46, 1834 (1992).
[14] D.R. Bowman et al., Phys. Rev. C52, 818 (1995).
[15] L. Phair et al., Nucl. Phys. A548, 489 (1992).
[16] L. Phair et al., Nucl. Phys. A564, 453 (1993).
[17] W.J. Llope et al., Phys. Rev. C51, 1325 (1995).
[18] J.P. Bondorf, et al., Phys. Rep. 257, 133 (1995).
[19] W. Bauer, Phys. Rev. C38, 1297 (1988).
[20] L. Phair et al., LBNL report 40778, accepted to Phys. Rev. Lett.
[21] D.W. Stracener et al., Nucl. Inst. & Meth. A 294, 485 (1990).